Acta Cryst. (1998). D**54**, 1353–1358

Structure of the Mutant E92K of [2Fe–2S] Ferredoxin I from *Spinacia oleracea* at 1.7 Å Resolution

Claudia Binda,[a] Alessandro Coda,[a] Alessandro Aliverti,[b] Giuliana Zanetti[b] and Andrea Mattevi[a]*

[a]*Dipartimento di Genetica e Microbiologia, Università di Pavia, via Abbiategrasso 207, 27100 Pavia, Italy, and* [b]*Dipartimento di Fisiologia e Biochimica Generali, Università degli Studi di Milano, via Celoria 26, 20133 Milano, Italy. E-mail: mattevi@ipvgen.unipv.it*

(*Received 12 February 1998; accepted 3 April 1998*)

Abstract

Ferredoxin I (Fd I) from *Spinacia oleracea* is composed of 97 amino-acid residues and a [2Fe–2S] cluster. The crystal structure of the E92K mutant of Fd I was solved by molecular replacement and refined to an *R* factor of 19.6% for 11755 reflections at 1.7 Å resolution. The overall structure and the active centre of spinach Fd is highly conserved with respect to ferredoxins of known structure. The E92K mutation appears to disturb a hydrogen-bond network which stabilizes the loop bearing the [2Fe–2S] cluster. This observation provides a rationale for the reduced electron-transfer efficiency displayed by the E92K mutant. Inspection of the crystal packing reveals that the side chain of Lys92 is engaged in an intermolecular interaction with Asp26 of a symmetry-related molecule. This feature may explain why only the mutant E92K and not wild-type Fd I could be successfully crystallized.

1. Introduction

Ferredoxin I (Fd I), a [2Fe–2S] iron–sulfur protein, is the major ferredoxin isoform present in the chloroplast, its biosynthesis being promoted by irradiation. Indeed, its function is directly related to photosynthesis (Knaff, 1996). Fd I is reduced by photosystem I, a light-dependent oxidoreductase that catalyses electron transfer between reduced plastocyanin and oxidized Fd I. Reduced Fd I then fulfils the outstanding role of distributing electrons of low redox potential to several metabolic pathways in the chloroplast. To this purpose, Fd I should be able to interact and form electron-transfer complexes with many different proteins. The three-dimensional structure of Fd I is of fundamental importance to clarify these interactions. The crystal structures of several cyanobacterial ferredoxins are known (Tsukihara *et al.*, 1990; Rypniewski *et al.*, 1991; Jacobson *et al.*, 1993; Fukuyama *et al.*, 1995). Although the three-dimensional structure of a plant ferredoxin, the *Equisetum arvense* Fd I, has been published recently (Ikemizu *et al.*, 1994), the most studied photosynthetic apparatus of higher plants is that from spinach, both from the physiological and the biochemical/structural points of view (Ort & Yocum, 1996). Thus, it was felt to be of considerable interest to undertake the crystallization of recombinant spinach Fd I, in order to provide a structural framework for the interpretation of the large amount of data on the spinach proteins present in the literature.

Here we report on the crystal structure of the mutant E92K of spinach Fd I at 1.7 Å resolution. The E92K mutant was produced in the framework of a protein-engineering study designed to investigate the role of the acidic cluster E92–E93–E94 in the interaction between Fd I and ferredoxin–$NADP^+$ reductase (Zanetti *et al.*, 1988; Aliverti *et al.*, 1995, 1997; Piubelli *et al.*, 1996). The three-dimensional structure of the E92K mutant supports the interpretation of these site-directed mutagenesis studies. Furthermore, the spinach Fd I structure will provide insights into the electron-transfer complex between Fd I and ferredoxin–$NADP^+$ reductase. The crystal structures of both the reductase purified from spinach leaves and that cloned and expressed in *Escherichia coli* have been determined at high resolution (Bruns & Karplus, 1995).

2. Materials and methods

2.1. *Crystallization and data collection*

Recombinant wild-type and mutant Fd I proteins were purified as described (Piubelli *et al.*, 1995). Screenings to identify crystallization conditions were performed using the wild-type protein and three mutants (E92K, E92A/E93A, E93A/E94A). The hanging-drop vapour-diffusion method was employed and various precipitants were tested, including ammonium sulfate, ammonium phosphate, polyethylene glycol and 2-methyl-2,4-pentanediol, within the pH range 4.5–8.5. The precipitant and protein solutions were mixed in a 1:1 ratio in the hanging drop and the experiments were performed both at 277 and 293 K.

The experiments with the wild type, E92A/E93A and E93A/E94A proteins produced small poorly shaped crystals which did not have any X-ray diffraction power. Conversely, the crystallization trials with the E92K mutant resulted in the growth of well ordered crystals.

© 1998 International Union of Crystallography
Printed in Great Britain – all rights reserved

ISSN 0907-4449 © 1998

Table 1. *Data-reduction and refinement statistics*

Number of observations	35600
Independent reflections	11755
Resolution limit (Å)	1.7
R_{merge} (%)†	7.8 (20.2)
Reflections >3σ (%)‡	93 (68)
Completeness (%)‡	97.6 (88.0)
Number of protein atoms	733
Number of solvent molecules	81
Final R factor	19.6
R_{free} (1000 reflections)	25.9
R.m.s. deviations from ideal values§	
Bond lengths (Å)	0.019
Bond angles (°)	2.994
Planar group (Å)	0.021
B factor, bonded atoms (Å^2)	5.1

† $R_{merge} = \sum_{hkl}\sum_i |I_i(hkl) - \langle I(hkl)\rangle| / \sum_{hkl}\sum_i I_i(hkl)$. ‡ The value for the highest resolution shell (1.8–1.7 Å) is given in parentheses. § The root-mean-square deviations from ideal values were calculated with the program *TNT* (Tronrud *et al.*, 1987).

These were obtained at 277 K using a precipitant solution containing 2.5–2.8 *M* ammonium sulfate in 50 m*M* potassium phosphate buffer pH 7.5. The best crystals were obtained when the protein was subjected to a hydrophobic interaction chromatography step immediately before crystallization. For this purpose, the protein was loaded onto a phenyl-Sepharose (Pharmacia) column and eluted in 1.3 *M* ammonium sulfate in 50 m*M* phosphate buffer pH 7.5. The eluted protein solution was concentrated to about 40 mg ml^{-1} without desalting and directly used for crystallization. Thus, the final crystallization protocol consisted of the following: droplets containing 40 mg ml^{-1} protein and 1.3 *M* ammonium sulfate in 50 m*M* phosphate buffer (pH 7.5) were equilibrated against a reservoir consisting of 2.6 *M* ammonium sulfate in 50 m*M* phosphate buffer (pH 7.5). In this way, crystals up to 0.5 × 0.5 × 1.0 mm were grown at 277 K in about 5 d.

Intensity data were collected at room temperature using a Rigaku R-AXIS image-plate detector mounted on a RU-200B rotating anode Cu $K\alpha$ X-ray generator equipped with a graphite monochromator. The crystals belong to the space group $P2_12_12_1$ with cell constants a = 31.0, b = 39.2, c = 83.5 Å and one molecule in the asymmetric unit. The data were evaluated with the program *MOSFLM* (Leslie, 1992), whereas the *CCP*4 suite of programs (Collaborative Computational Project, Number 4, 1994) was used for data reduction. A total of 11755 independent reflections were measured resulting in a 97% complete data set up to 1.7 Å resolution. Data-collection and processing statistics are summarized in Table 1.

2.2. *Structure solution and refinement*

The crystal structure of the E92K Fd I mutant was solved by the molecular-replacement method (Rossmann & Blow, 1962) using the program *AMoRe* (Navaza, 1994). Since *E. arvense* Fd I shares 57% sequence identity with spinach Fd I (Ikemizu *et al.*, 1994), it was chosen as the search model for molecular replacement. Both rotation-function and translation-function calculations produced clear solutions (first peak at 6σ above the mean in both functions) and were of unambiguous interpretation. Using the properly oriented and translated model, an R factor of 44.8% was calculated for data to 3.5 Å resolution. After rigid-body refinement, the R factor decreased to 43.7% with a correlation coefficient of 0.51.

The initial E92K Fd I model was built with *O* (Jones *et al.*, 1991) using the Cα positions of the model derived from rigid-body refinement. The restrained least-

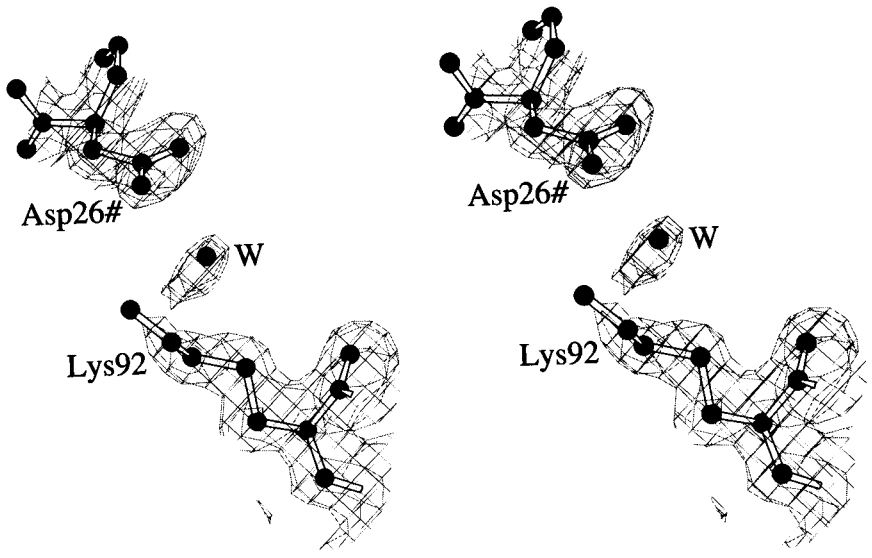

Fig. 1. Final $2F_o - F_c$ map of intermolecular crystal contact between Lys92 and Asp26. The symbol # indicates that the residue belongs to a symmetry-related molecule. 'W' is used to label an ordered water molecule.

Table 2. *Comparison between E92K spinach Fd I and other ferredoxins*

Species†	Resolution (Å)	Number of residues	Superposed residues‡	Sequence identity (superposed residues)	R.m.s. deviation (Å)
A. sacrum	2.2	96	1–60, 71–91	64%	0.66
Anabaena§	2.5	98	1–8, 13–96	67%	0.65
Anabaena¶	1.7	98	1–8, 13–96	48%	0.56
E. arvense	1.8	95	2–8, 13–92	57%	0.54
S. platensis	2.5	98	2–8, 13–92	68%	0.60

† The comparison was made by superposing onto the E92K Cα atoms the following ferredoxins of known crystal structure: *Aphanothece sacrum* (Tsukihara *et al.*, 1990) at 1.7 Å, *Anabaena* 7120 vegetative cell at 2.5 Å (Rypniewski *et al.*, 1991), *Anabaena* 7120 heterocyst cell at 1.7 Å (Jacobson *et al.*, 1993), *E. arvense* at 1.8 Å (Ikemizu *et al.*, 1994) and *Spirulina platensis* at 2.5 Å (Fukuyama *et al.*, 1995). For a sequence comparison among these ferredoxins see Fig. 4(*a*). ‡ Residue numbering of spinach Fd I. Residues 8–12 were excluded from the superpositions because they are part of a solvent-exposed loop which presents insertions and/or deletions among the various ferredoxin sequences. § Vegetative cell. ¶ Heterocyst cell.

squares program *TNT* (Tronrud *et al.*, 1987) was employed for the crystallographic refinement. All data were used (no σ or low-resolution cut-off), except for 1000 randomly chosen reflections excluded in order to calculate $R_{\rm free}$ (Brünger, 1992). During refinement, no geometric restraints were imposed on the atoms of the [2Fe–2S] cluster. Water molecules were added if they had suitable stereochemistry and well defined electron-density peaks in both $2F_o - F_c$ and $F_o - F_c$ maps. At the end of the refinement, a final cycle was carried out using all reflections, including those set aside for the calculation of $R_{\rm free}$. The resulting coordinates were taken as the final model used for structure analysis (Table 1). Atomic coordinates and structure factors have been deposited with the Protein Data Bank (Bernstein *et al.*, 1977).†

The hydrogen-bond contacts and the stereochemistry of the structure were monitored by the program *PROCHECK* (Laskowski *et al.*, 1993). Structure superpositions were performed by the *CCP*4 suite of programs (Collaborative Computational Project, Number 4, 1994). The drawings were generated with the program *MOLSCRIPT* (Kraulis, 1991).

3. Results and discussion

3.1. *Overall structure and the [2Fe–2S] cluster region*

The final model of E92K spinach Fd I has an *R* factor of 19.6% for 11755 reflections to 1.7 Å resolution. It contains coordinates for all 97 amino-acid residues (733 non-H atoms), plus the [2Fe–2S] cluster atoms and 81 solvent molecules. All residues fit well to the final $2F_o - F_c$ map (Fig. 1), except for the side chains of Glu15, Lys50, Lys52, Glu94 and the Nζ atom of Lys92, which lack clear density. The Ramachandran plot shows 87.1% of the residues in most favoured regions and 12.9% residues in additional allowed regions (Laskowski *et al.*, 1993), with no residues in energetically unfavourable conformations (Fig. 2). The stereochemical parameters of the final model of the E92K Fd I structure are listed in Table 1.

The spinach Fd I structure is characterized by a central core formed by a five-stranded β-sheet (β1–β5) and an α-helix (α1) laying on top of the sheet (Fig. 3). This particular structure is called a 'β-grasp' motif and it is found in several functionally unrelated proteins (Fukuyama *et al.*, 1995; Orengo *et al.*, 1997). In addition, there are two short β-strands (β1′ and β2′), an α-helix (α2) and a short C-terminal helical turn (α3). In this respect, the structure of spinach Fd I is very similar to those of the other five plant-type ferredoxins of known crystal structure (Figs. 4*a* and 4*b*). There are only two regions which show significant conformational differences: the loop 8–13 (spinach Fd I numbering), whose length varies because of insertions or deletions (Figs. 4*a* and 4*b*) and the C-terminal residues 93–98 which adopt a

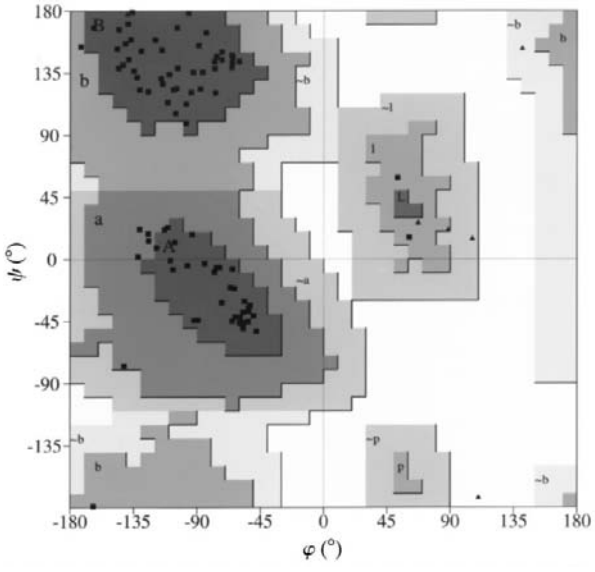

Fig. 2. Ramachandran plot of the E92K mutant of spinach Fd I, produced with *PROCHECK* (Laskowski *et al.*, 1993).

† Atomic coordinates and structure factors have been deposited with the Protein Data Bank, Brookhaven National Laboratory (Reference: 1A70 and R1A70SF).

Table 3. *Bond-length distances in the [2Fe–2S] cluster*

Species†	Fe1—S1	Fe1—S2	Fe1—S$^{\gamma}$39	Fe1—S$^{\gamma}$44	Fe2—S1	Fe2—S2	Fe2—S$^{\gamma}$47	Fe2—S$^{\gamma}$77
S. oleracea	2.28	2.27	2.32	2.28	2.22	2.31	2.36	2.27
A. sacrum	2.25	2.18	2.26	2.31	2.20	2.19	2.26	2.32
Anabaena‡	2.19	2.23	2.33	2.35	2.19	2.23	2.22	2.10
Anabaena§	2.21	2.17	2.29	2.28	2.19	2.20	2.32	2.26
E. arvense	2.17	2.22	2.31	2.24	2.26	2.24	2.26	2.28
S. platensis	2.17	2.20	2.28	2.26	2.23	2.22	2.26	2.27
R.m.s. (Å)¶	0.04	0.03	0.02	0.04	0.03	0.04	0.05	0.07

† The comparison was made with the ferredoxins of known crystals structure: *Aphanothece sacrum* (Tsukihara *et al.*, 1990) at 1.7 Å, *Anabaena* 7120 vegetative cell at 2.5 Å (Rypniewski *et al.*, 1991), *Anabaena* 7120 heterocyst cell at 1.7 Å (Jacobson *et al.*, 1993), *E. arvense* at 1.8 Å (Ikemizu *et al.*, 1994) and *S. platensis* at 2.5 Å (Fukuyama *et al.*, 1995). ‡ Vegetative cell. § Heterocyst cell. ¶ R.m.s. deviations for the distances observed in the six ferredoxin structures.

different conformation in the *Equisetum arvense* protein. The strong conservation of the ferredoxin fold is highlighted by superposition of the homologous Cα atoms, which produced r.m.s. deviations below 0.7 Å in all cases (Table 2).

The similarity of spinach Fd I to the other ferredoxins is evident in the region comprising the iron–sulfur centre (Table 3). The cluster lies in a solvent-exposed pocket formed by the loop connecting α1 with β3 (Figs. 3 and 5*a*). This loop bears three (Cys39, Cys44, Cys47) of the four cysteine residues that coordinate the two Fe atoms (Figs. 4*b* and 5*b*). The stereochemistry of the cluster is virtually identical to that of the other ferredoxins, as the differences in the Fe—S distances are within the range of the coordinate error (Table 3). In particular, the orientation of the cluster is such that the Fe1 atom is more exposed to solvent whereas Fe2 is positioned within the protein interior. The differences in the chemical environment of the two Fe atoms are functionally relevant, since the more hydrophilic environment of Fe1 is thought to favour the localization on Fe1 of the additional electron which is taken up by the cluster upon protein reduction (Tsukihara *et al.*, 1990; Skijeldal *et al.*, 1991; Fu *et al.*, 1992).

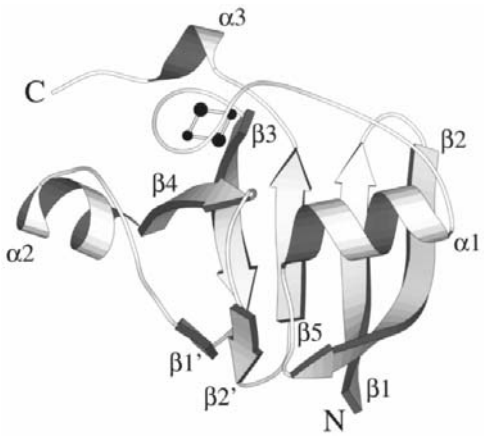

Fig. 3. Ribbon diagram of the E92K Fd I structure. In this orientation, the β-grasp motif characterizing the architecture of the protein is visible. The cluster is in the upper-left corner. For the sake of clarity, the cysteine residues coordinating the Fe atoms are not represented. The letters 'N' and 'C' identify the position of the N- and C-terminus, respectively.

3.2. *Crystal-packing interactions and the successful crystallization of the E92K mutant*

The E92K mutant was the only form of spinach Fd I which produced crystals useful for structure determination. Despite many attempts, no crystals were obtained of the wild-type E92A/E93A and E93A/E94A proteins. Inspection of the crystal packing of the E92K structure shows that the Lys92 side chain is located in proximity to Asp26 of a symmetry-related molecule (distance between Lys92 C$^{\varepsilon}$ and Asp26 O$^{\delta 1}$ of 3.5 Å; Fig. 1). The terminal amino group of the Lys92 side chain is not visible in density, possibly because of disorder (Fig. 1). However, the proximity of Lys92 to Asp26 suggests that a favourable electrostatic contact may exist between the two oppositely charged residues. Such an intermolecular interaction cannot be formed in the E92A/E93A mutant, whereas crystal packing would lead to unfavourable contact between Glu92 and Asp26 in the case of the wild-type and E93A/E94A proteins. These observations might explain why only the E92K mutant produced crystals. However, it must be recalled that the E92K crystals were grown at high salt concentration, which increases the dielectric constant of the medium and weakens the electrostatic interactions. Therefore, it cannot be ruled out that, in addition to the formation of the Lys92–Asp26 intermolecular contact, other unknown factors are responsible for the inability of the wild type and the double mutants to crystallize.

3.3. *The site of the E92K mutation*

Cyclic voltammetry and EPR measurements (Aliverti *et al.*, 1995) revealed that the E92K mutation increases the redox potential by 93 mV (from −401 mV to −308 mV) with respect to the wild type. Furthermore, the E92K mutant displays a reduced efficiency in transferring electrons from photosystem I to ferredoxin–NADP^{+} reductase (Piubelli *et al.*, 1996). Inspection of the three-dimensional structure (Figs. 5*a* and 5*b*) reveals

that Lys92 is positioned on the α3 helix (Fig. 3) at a distance of 9.0 Å from Fe1 and 3.9 Å from the O^{γ} of Ser46, which is hydrogen bonded (3.6 Å) to S^{γ} of Cys44 in the cluster (Fig. 5*b*).

Glu92 of spinach Fd I is homologous to Glu94 of *Anabaena* vegetative-cell ferredoxin (Fig. 4*b*). Recently, the three-dimensional structure of the E94K mutant of *Anabaena* Fd has been reported (Hurley *et al.*, 1997) and compared with the known structure of the wild-type protein. As in spinach Fd I and also in *Anabaena* protein, the mutation causes a substantial increase in the redox potential (80 mV). X-ray analysis of the E94K mutant of *Anabaena* ferredoxin (Hurley *et al.*, 1997) shows that the mutation does not induce any significant conformational change in the overall structure of the protein. However, the introduction of the lysine side chain causes the loss of the hydrogen bond, which in the wild-type protein is formed between Glu94 and Ser47 (homologous to Ser45 of spinach Fd I; Figs. 4*b* and 5*b*). This interaction is thought to have a key role in the stabilization of the loop carrying the [2Fe–2S] cluster. Modelling of a glutamate residue in position 92 of spinach Fd I shows that the acidic side chain would be well positioned to interact with Ser45. Thus, it is conceivable that Glu92 of the wild-type spinach protein is engaged in a hydrogen bond with Ser45, in a similar fashion as in the *Anabaena* ferredoxin. Therefore, the new geometry of the hydrogen-bond network, together with the elimination of a negative charge in the vicinity of the iron–sulfur cluster, seems the likely cause of the increase of the E92K mutant redox potential.

The E92K mutation makes ferredoxin less efficient in donating electrons to $NADP^+$ through the ferredoxin–$NADP^+$ reductase in the physiological reaction, whereas the electron-transfer capacity in the reverse direction is increased (Piubelli *et al.*, 1996; Aliverti *et al.*, 1997). Homology-modelling studies based on the structure of phthalate dioxygenase reductase suggest that residue 92 is unlikely to be directly involved in the interactions between Fd and ferredoxin–$NADP^+$ reductase (Correll *et al.*, 1993). On the other hand, the similarity between the structure of the E92K mutant and that of the other ferredoxins implies that the mutation does not induce substantial structural changes that could be responsible for a less favourable interaction of the mutant Fd I with the reductase. Thus, on the basis of the E92K Fd I structure, it can be inferred that the increase of redox potential is the most important cause of the altered

```
                        β1          β2        α1
                     eeeeeeee    eeeeeeee  hhhhhhhhh                ee
S. oleracea          AAYKVTLVT-PTG-NVEFQCPDDVYILDAAEEEGIDLPYSCRAGSCSSCA 48
A. sacrum            ASYKVTLKT-PDG-DNVITVPDDEYILDVAEEEGLDLPYSCRAGACSTCA
Anabaena (vegetative) ATFKVTLINEAEGTKHEIEVPDDEYILDAAEEQGYDLPFSCRAGACSTCA
Anabaena (heterocyst) ASYQVRLINKKQDIDTTIEIDEETTILDGAEENGIELPFSCHSGSCSSCV
E. arvense           -AYKTVLKT-PSG-EFTLDVPEGTTILDAAEEAGYDLPFSCRAGACSSCL
S. platensis          ATYKVTLINEAEGINETIDCDDDTYILDAAEEAGLDLPYSCRAGACSTCA
                                                      *    *  *

                     β3    β1′          α2   β4     β2′    β5    α3
                     eeeee eee       hhhhhhheeeee   eee  eeeee  hhhh
S. oleracea          GKLKTGSLNQDDQSFLDDDQIDEGWVLTCAAYPVSDVTIETHKEEELTA  97
A. sacrum            GKLVSGPAPDEDQSFLDDDQIQAGYILTCVAYPTGDCVIETHKEEALY-
Anabaena (vegetative) GKLVSGTVDQSDQSFLDDDQIEAGYVLTCVAYPTSDVVIQTHKEEDLY-
Anabaena (heterocyst) GKVVEGEVDQSDQIFLDDEQMGKGFALLCVTYPRSNCTIKTHQEPYLA-
E. arvense           GKVVSGSVDESEGSFLDDGQMEEGFVLTCIAIPESDLVIETHKEEELF-
S. platensis          GTITSGTIDQSDQSFLDDDQIEAGYVLTCVAYPTSDCTIKTHQEEGLY-
                                             *
```

(*a*)

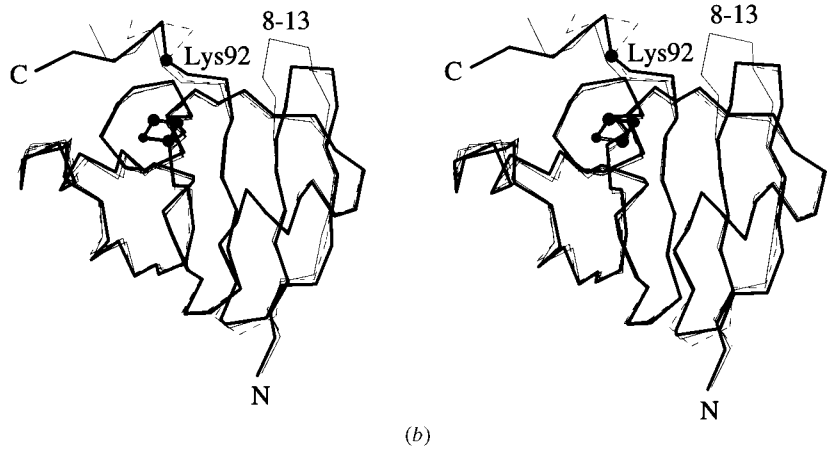

(*b*)

Fig. 4. (*a*) Alignment of six plant-type ferredoxins of known crystal structure (see Table 2). Residues belonging to α-helices and β-strands are indicated by the letters 'h' and 'e', respectively (the secondary structures are referred to E92K spinach Fd I). The cysteine residues which coordinate the Fe atoms are indicated by an asterisk. (*b*) Stereoview of the superposition (see Table 2) of the structures of E92K spinach Fd I (thick line), *Anabaena* vegetative-cell Fd (thin line) and *E. arvense* Fd (dashed line). Lys92 and the loop formed by residues 8–13 are labelled.

functional properties of the E92K mutant. Better insights into the protein–protein interaction must await the resolution of the three-dimensional structure of the complex between Fd I and ferredoxin–NADP$^+$ reductase, which is being pursued in our laboratory by two different routes: by attempting crystallization of both the dissociable complex at low ionic strength and of the chimeric protein comprising Fd and ferredoxin–NADP$^+$ reductase in a single polypeptide chain, as obtained by gene fusion (Aliverti & Zanetti, 1997).

This work was supported by grants from Ministero per l'Università e la Ricerca Scientifica e Tecnologica (to GZ and AC), Consiglio Nazionale delle Ricerche (No. 96.04941.74 to AM and No. 97.04418 to GZ) and Agenzia Spaziale Italiana (No. ASI-ARS-96-191).

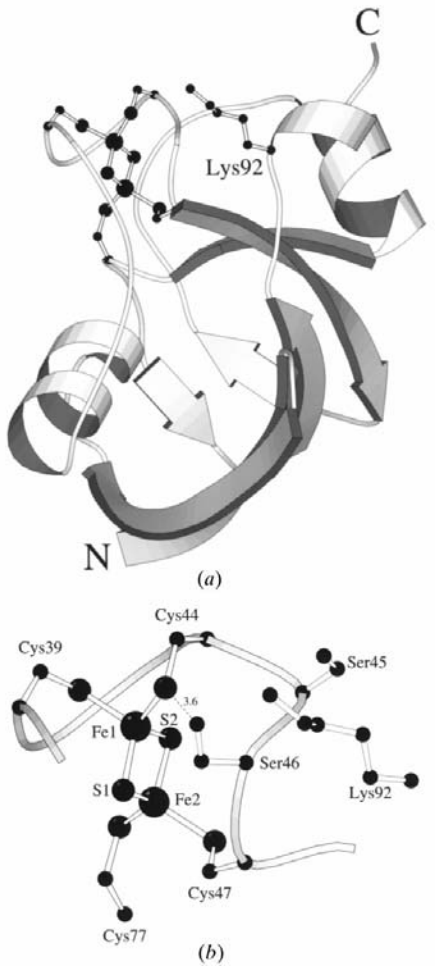

Fig. 5. (*a*) Overall structure of Fd I highlighting the position of Lys92 with respect to the [2Fe–2S] cluster. The view is rotated by approximately 90° about the vertical axis with respect to Fig. 3. (*b*) The [2Fe–2S] cluster represented in the same orientation as in Fig. 5(*a*). The interatomic distances between the amino group of Lys92 and the hydroxyl atoms of Ser45 and Ser46, respectively, and the hydrogen-bond distance between $O^{\gamma}46$ and $S^{\gamma}44$ are indicated in Å (see text).

References

Aliverti, A., Hagen, W. R., & Zanetti, G. (1995). *FEBS Lett.* **368**, 220–224.
Aliverti, A., Livraghi, A., Piubelli, L. & Zanetti, G. (1997). *Biochim. Biophys. Acta*, **1342**, 45–50.
Aliverti, A. & Zanetti, G. (1997). *Biochemistry*, **36**, 14771–14777.
Bernstein, F. C., Koetzle, T. F., Williams, G. J. B., Meyer, E. F. Jr, Brice, M. D., Rodgers, J. R., Kennard, O., Shimanouchi, T. & Tasumi, M. (1977). *J. Mol. Biol.* **112**, 535–542.
Brünger, A. T. (1992). *Nature (London)*, **355**, 472–475.
Bruns, C. M. & Karplus, P. A. (1995). *J. Mol. Biol.* **247**, 125–145.
Collaborative Computational Project, Number 4 (1994). *Acta Cryst.* D**50**, 760–767.
Correll, C. C., Ludwig, M. L., Bruns, C. M. & Karplus, A. (1993). *Protein Sci.* **2**, 2112–2133.
Fu, W., Drozdzewski, P. M., Davies, M. D., Sligar, S. G. & Johnson, M. K. (1992). *J. Biol. Chem.* **267**, 15502–15510.
Fukuyama, K., Ueki, N., Nakamura, H., Tsukihara, T. & Matsubara, H. (1995). *J. Biochem.* **117**, 1017–1023.
Hurley, J. K., Weber-Main, A. M., Stankovich, M. T., Benning, M. M., Thoden, J. B., Vanhooke, J. L., Holden, H. M., Kee Chae, Y., Xia, B., Cheng, H., Markley, J. L., Martinez-Júlvez, M., Gómez-Moreno, C., Schmeits, J. L. & Tollin, G. (1997). *Biochemistry*, **36**, 11100–11117.
Ikemizu, S., Bando, M., Sato, T., Morimoto, Y., Tsukihara, T. & Fukuyama, K. (1994). *Acta Cryst.* D**50**, 167–174.
Jacobson, B. L., Chae, Y. K., Markley, J. L., Rayment, I. & Holden, H. M. (1993). *Biochemistry*, **32**, 6788–6793.
Jones, T. A., Zou, J. Y., Cowan, S. W. & Kjeldgaard, M. (1991). *Acta Cryst.* A**47**, 110–119.
Knaff, D. B. (1996). *Oxygenic Photosynthesis: The Light Reactions*, Vol. 4, edited by D. R. Ort & C. F. Yocum, pp. 333–361. Dordrecht: Kluwer.
Kraulis, P. J. (1991). *J. Appl. Cryst.* **24**, 946–950.
Laskowski, R. A., MacArthur, M. W., Moss, D. S. & Thornton, J. M. (1993). *J. Appl. Cryst.* **26**, 283–291.
Leslie, A. G. W. (1992). *Joint CCP4 and ESF-EACMB Newsletter: Protein Crystallography*, No. 26. Warrington: Daresbury Laboratory.
Navaza, J. (1994). *Acta Cryst.* A**50**, 157–163.
Orengo, C. A., Michie, A. D., Jones, S., Jones, D. T., Swindels, M. B. & Thornton, G. M. (1997). *Structure*, **5**, 1093–1108.
Ort, D. R. & Yocum, C. F. (1996). Editors. *Oxygenic Photosynthesis: The Light Reactions*, Vol. 4. Dordrecht: Kluwer.
Piubelli, L., Aliverti, A., Bellintani, F. & Zanetti, G. (1995). *Protein Exp. Purif.* **6**, 298–304.
Piubelli, L., Aliverti, A., Bellintani, F. & Zanetti, G. (1996). *Eur. J. Biochem.* **236**, 465–469.
Rossmann, M. G. & Blow, D. M. (1962). *Acta Cryst.* **15**, 24–31.
Rypniewski, W. R., Breiter, D. R., Benning, M. M., Wesenberg, G., Oh, B. H., Markley, J. L., Rayment, I. & Holden, H. M. (1991). *Biochemistry*, **30**, 4126–4131.
Skijeldal, L., Westler, W. M., Oh, B.-H., Krezel, A. M., Holden, H. M., Jacobson, B. L., Rayment, I. & Markley, J. L. (1991). *Biochemistry*, **30**, 7363–7368.
Tronrud, D. E., Ten Eyck, L. F. & Matthews, B. W. (1987). *Acta Cryst.* A**43**, 489–501.
Tsukihara, T., Fukuyama, K., Mitzushima, M., Harioka, T., Kusunoki, M., Katsube, Y., Hase, T. & Matsubara, H. (1990). *J. Mol. Biol.* **216**, 399–410.
Zanetti, G., Morelli, D., Ronchi, S., Negri, A., Aliverti, A. & Curti, B. (1988). *Biochemistry*, **27**, 3753–3759.